Journal of Sound and Vibration (1997) **200**(3), 327–345

COMPLEX MODAL ANALYSIS OF A FLEXURAL VIBRATING BEAM WITH VISCOUS END CONDITIONS

G. Oliveto

Istituto di Scienza della Costruzioni, *Università di Catania*, *Viale Andrea Doria* 6, 95125 *Catania*, *Italy*

AND

A. Santini and E. Tripodi

Instituto di Ingegneria Civile ed Energetica, *Università di Reggio Calabria*, *Via Emilio Cuzzocrea* 48, 89128 *Reggio Calabria*, *Italy*

(*Received* 12 *February* 1996, *and in final form* 5 *August* 1996)

The complex mode superposition method for the dynamical analysis of a simply supported beam with two rotational viscous dampers attached at its end is presented. First, a numerical procedure for the evaluation of complex frequencies and modes of vibration has been worked out. Second, the appropriate orthogonality conditions have been established in order to decouple the equation of motion. The complex mode superposition method has then been used for the dynamic analysis in the time and frequency domains. Finally, some numerical applications, under impulsive and harmonic transverse accelerations of both ends, have been reported in order to illustrate the effects of the dampers on the response amplitude.

1. INTRODUCTION

Dampers are frequently used in the design of structures under dynamic and seismic excitations. These devices are employed not only in the field of vibration isolation, but also in that of the passive and active control of the dynamic response. Their aim is to dissipate part of the vibration energy and for this reason they lead to a reduction in the response amplitude.

In the dynamic response analysis of systems with viscous dampers it should be taken into account that, due to the presence of such devices, the damping is non-classical [1]. As a consequence, the dynamic analysis cannot be carried out by the standard mode superposition method. In fact, natural frequencies and modes of vibration are complex and the equations of motion have to be decoupled in the complex domain.

This technique has been clearly stated for discrete multi-degree-of-freedom systems and the physical meaning of all of the elements that define the solutions has been elucidated [1]. This method has recently been extended, by two of the present authors, to distributed parameter systems, in the study of two simple models for dynamic soil–structure interaction [2–4].

However, the applicability of the complex modal analysis for distributed parameter systems is limited by the lack of general procedures for the evaluation of complex frequencies and modes of vibration. For a longitudinally vibrating cantilever beam with

0022–460X/97/080327 + 19 $25.00/0/sv960717

a viscous dashpot attached at its free end, the complex frequencies and modes of vibration can be evaluated in closed form [5, 6]. For such a system a method for the dynamic analysis based on the use of complex modes of vibration has also been proposed [6]. Some results in terms of complex frequencies and modes have also been provided for flexural vibrating beams with general end conditions [7], but without explicit directions about the numerical procedures used for their evaluation.

The aim of this paper is to apply the complex mode superposition method to the dynamic analysis of a Bernoulli–Euler simply supported beam with two rotational viscous dampers attached at its ends.

For this system a numerical procedure for the evaluation of complex frequencies and modes of vibration has been developed and the orthogonality conditions, which allow the decoupling of the equation of motion in terms of principal co-ordinates, have been derived. A parametric study has then been carried out in order to investigate how the natural frequencies depend on the dynamic characteristics of the system. Subsequently, some numerical applications, under impulsive and harmonic transverse accelerations acting simultaneously at both ends, have been reported and a comparison has been made with the response of the same beam without dampers. Finally, it has been shown how, by selecting appropriately the properties of the beam and the dampers, a considerable abatement of the structural response can be obtained.

2. THE STRUCTURAL SYSTEM

The system under investigation is composed of a uniform simply supported Bernoulli–Euler beam with two rotational viscous dampers, with damping constant c, attached at its end, see Figure 1. The beam has length L, mass per unit length m and flexural rigidity EJ.

3. THE GOVERNING EQUATIONS

The governing equations of the present problem are the equation of motion for the Bernoulli–Euler beam and the corresponding boundary conditions. For vertical ground excitations the equation of motion takes the form

$$EJ\,\partial^4 v(z,t)/\partial z^4 + m\,\partial^2 v(z,t)/\partial t^2 = -m\,\partial^2 v_g(t)/\partial t^2, \tag{1}$$

where $v(z,t)$ is the vertical displacement and $v_g(t)$ represents the ground vertical displacement. The boundary conditions at the two ends of the beam are defined in terms of displacements and bending moments as

$$v(0,t) = 0, \qquad v(L,t) = 0, \tag{2a, b}$$

$$M(0,t) = -c\,\partial^2 v(0,t)/\partial z\,\partial t, \qquad M(L,t) = c\,\partial^2 v(L,t)/\partial z\,\partial t. \tag{3a, b}$$

where

$$M(z,t) = -EJ\,\partial^2 v(z,t)/\partial z^2. \tag{4}$$

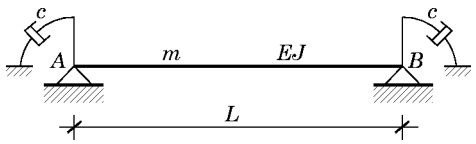

Figure 1. The structural system.

For harmonic motions the end moments and rotations may be written in the forms

$$M(0, t) = -M_A \exp\{i\omega t\}, \qquad M(L, t) = M_B \exp\{i\omega t\},$$
$$\varphi(0, t) = \varphi_A \exp\{i\omega t\}, \qquad \varphi(L, t) = \varphi_B \exp\{i\omega t\}, \tag{5a–d}$$

where, M_A, M_B, φ_A and φ_B are positive when the direction of rotation is counterclockwise.

4. DYNAMIC STIFFNESS MATRIX

The dynamic stiffness matrix for the simply supported beam may be derived from the equation of motion (1) and appropriate boundary conditions through standard methods of structural dynamics [8] in the form

$$\begin{bmatrix} M_A \\ M_B \end{bmatrix} = \frac{EJ}{L} \begin{bmatrix} \alpha & \bar{\alpha} \\ \bar{\alpha} & \alpha \end{bmatrix} \begin{bmatrix} \varphi_A \\ \varphi_B \end{bmatrix} \tag{6}$$

where

$$\alpha = \frac{\sin b \cosh b - \cos b \sinh b}{1 - \cos b \cosh b} b, \qquad \bar{\alpha} = \frac{\sinh b - \sin b}{1 - \cos b \cosh b} b, \tag{7a, b}$$

are stiffness coefficients which depend on the frequency parameter $b = aL$, in which

$$a^4 = (m/EJ)\omega^2. \tag{8}$$

In the case of the beam with dampers, since for harmonic motions

$$\begin{bmatrix} M_A \\ M_B \end{bmatrix} = -i\omega c \begin{bmatrix} \varphi_A \\ \varphi_B \end{bmatrix}, \tag{9}$$

one obtains

$$\begin{bmatrix} 0 \\ 0 \end{bmatrix} = \frac{EJ}{L} \begin{bmatrix} \alpha + i\mu b^2 & \bar{\alpha} \\ \bar{\alpha} & \alpha + i\mu b^2 \end{bmatrix} \begin{bmatrix} \varphi_A \\ \varphi_B \end{bmatrix}, \tag{10}$$

where $\mu = c/L\sqrt{mEJ}$ is a structural parameter. Therefore, the dynamic stiffness matrix takes the form

$$\mathbf{K} = \frac{EJ}{L} \begin{bmatrix} \alpha + i\mu b^2 & \bar{\alpha} \\ \bar{\alpha} & \alpha + i\mu b^2 \end{bmatrix}, \tag{11}$$

where the term $i\mu b^2$ accounts for the viscous damper effects.

5. NATURAL FREQUENCIES

The natural frequencies of the system are obtained by setting to zero the determinant of the dynamic stiffness matrix. This condition provides the two equations

$$\alpha \mp \bar{\alpha} + i\mu b^2 = 0, \tag{12}$$

where the frequency parameter b^2 is complex in general. By setting

$$b^2 = p + iq, \tag{13}$$

simple algebraic manipulations lead to

$$(A \mp B - \mu q) + \mathrm{i}(C \mp D + \mu p) = 0, \tag{14}$$

where A, B, C and D are real functions of p and q, the expressions for which are reported in Appendix A. The natural frequency parameters of the system are given by the values of p and q, which are simultaneously solutions of the real and the imaginary part of equations (14). This condition leads to the following two systems of equations

$$\left.\begin{matrix} A - B - \mu q = 0 \\ C - D + \mu p = 0 \end{matrix}\right\}, \qquad \left.\begin{matrix} A + B - \mu q = 0 \\ C + D + \mu p = 0 \end{matrix}\right\}. \tag{15, 16}$$

By analogy with the simply supported beam, for which the odd frequencies are given by the equation $\alpha - \bar{\alpha} = 0$ and the even ones by the equation $\alpha + \bar{\alpha} = 0$, the couples (p_n, q_n) which are solutions of the system (15) correspond to the dimensionless natural frequencies of odd order, while the couples (p_n, q_n) which are solutions of the system (16) correspond to the even order ones. Because the functions A, B, C and D are even in p, if the couple (p_n, q_n) is a solution of the system (15) or of the system (16), so is the couple $(-p_n, q_n)$. The complex natural frequencies are, then, given by the relationship

$$\omega_n = b_n^2 \sqrt{EJ/mL^4} = (\pm p_n + \mathrm{i}q_n)\sqrt{EJ/mL^4}. \tag{17}$$

By considering the modulus

$$|\omega_n| = \sqrt{(p_n^2 + q_n^2)EJ/mL^2} \tag{18}$$

and defining the modal damping ratios

$$\xi_n = q_n/\sqrt{(p_n^2 + q_n^2)}, \tag{19}$$

the natural frequencies may be written as

$$\omega_n = |\omega_n|(\pm\sqrt{1 - \xi_n^2} + \mathrm{i}\xi_n). \tag{20}$$

The real part of ω_n therefore has the physical meaning of the damped natural frequency of a single-degree-of-freedom viscous linear system with natural frequency $|\omega_n|$ and damping ratio ξ_n. Due to its dependence on the damping parameter q_n, the natural frequency $|\omega_n|$ is not equal to the natural frequency of the corresponding damped system and, for this reason, is termed the nth pseudo-undamped natural frequency [1]. It should be noticed that the damping parameter

$$q_n = \xi_n |\omega_n| \tag{21}$$

cannot, obviously, be negative.

5.1. EVALUATION OF THE NATURAL FREQUENCIES

For each selected value of the structural parameter μ, the natural frequencies are given by the values of p and q which simultaneously satisfy the equations of the system (15) or those of the system (16). By dividing the first of these equations by the second and after some algebraic manipulations, one obtains

$$q = -p(A \mp B)/(C \mp D), \tag{22}$$

where the minus sign refers to system (15), while the plus sign refers to system (16). It may be noticed that this equation is independent of μ and the couples (p, q) which are its solutions represent all the admissible solutions of the frequency equation (14). By selecting

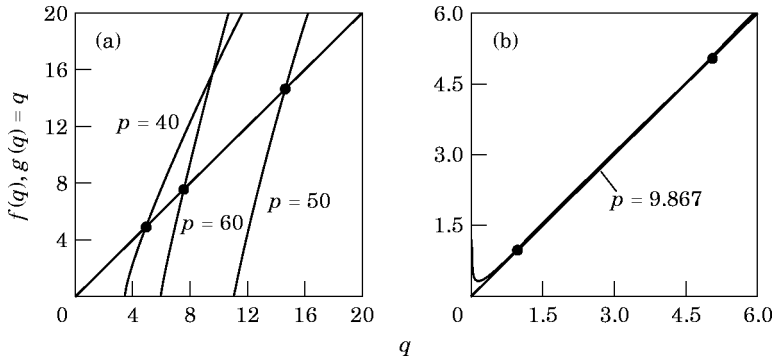

Figure 2. Evaluations of admissible solutions.

any value of p and taking into account that q cannot be negative, these couples may be obtained by the intersection of the straight line

$$f(q) = q, \tag{23}$$

and the curve

$$g(q) = -p(A \mp B)/(C \mp D). \tag{24}$$

For example, some admissible solutions are evaluated in Figures 2(a) and 2(b) for some values of p.

In the plane p–q such couples describe a countable infinity of curves of which the first five are reported in Figure 3. Each of them refers to a natural frequency. For each point of these curves the corresponding μ may be derived from any of the two equations of the system (15) or of the system (16). For example, considering the first equation, one obtains

$$\mu = (A \mp B)/q. \tag{25}$$

It should be noticed that the points of each curve are in a one-to-one correspondence with the values of μ in the interval $[0, \infty]$. In particular, the points which lie on the p-axis are related to the values $\mu = 0$ and $\mu = \infty$ of the structural parameter. For each curve, the smaller value coincides with a dimensionless natural frequency, p_{ss}, of the simply supported beam, while the larger one is associated with the frequency, p_{cc}, of the beam with clamped ends. In fact, as can easily be proved, the frequency equations of the simply supported beam and of the beam with clamped ends may be obtained as limiting cases from equation

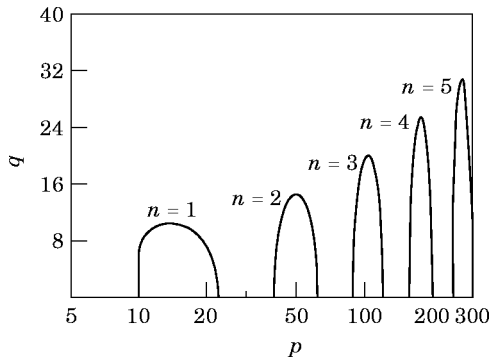

Figure 3. Admissible solutions of the frequency equation for the first five natural frequencies.

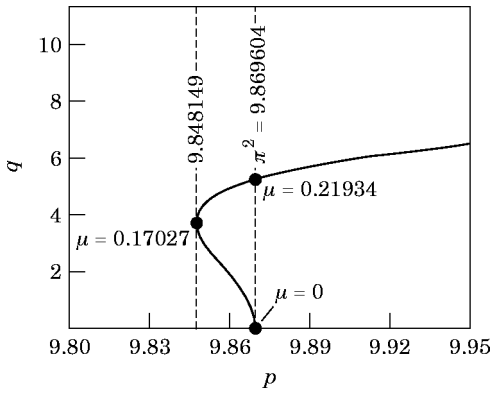

Figure 4. Admissible solutions of the frequency equation for the first natural frequency: detail in close proximity to the first natural frequency of the beam without dampers.

(14) for $\mu \to 0$ and for $\mu \to \infty$. Moreover, all of the other points correspond to distinct values of μ within the interval $[0, \infty]$. It may also be noticed that, for all the curves but the first one, as μ increases from zero to infinity p increases from p_{ss} to p_{cc}.

For the first natural frequency the curve presents a different trend, as is shown by Figure 4. As μ increases from zero, at first p decreases, attaining its minimum values, $p_{min} = 9{\cdot}848149$, for $\mu = 0{\cdot}17027$. Subsequently, for $\mu > 0{\cdot}17027$, p increases monotonically up to p_{cc}.

The straight line $f(q)$ and the curve $g(q)$ have, therefore, only one intersection in the interval $]p_{ss}, p_{cc}]$, as may be seen in Figure 2(a). For the first natural frequency there are two intersections in the interval $]p_{min}, p_{ss}]$; see Figure 2(b). The first one refers to a value of μ within the interval $0 \leqslant \mu < 0{\cdot}17027$, while the second one to a value of μ within the interval $0{\cdot}17027 < \mu < 0{\cdot}21934$. Therefore, for any frequency and for any value of the structural parameter μ, an interval is defined in which p must stay. Because in this interval the frequency equation has only one solution, this can easily be found by means of a bisection procedure. For the first frequency, the actual value of the structural parameter μ decides whether p_{ss} is the upper bound p_u or the lower bound p_l for p. For $\mu < 0{\cdot}17027$, then, it is $p_l = p_{min} = 9{\cdot}848149$ and $p_u = p_{ss} = \pi^2$, while for $\mu > 0{\cdot}17027$ it may be set to $p_l = p_{min}$ and $p_u = p_{cc}$. For all higher frequencies it is $p_l = p_{ss}$ and $p_u = p_{cc}$. A trial value for p may be chosen as

$$\hat{p} = (p_l + p_u)/2 \tag{26}$$

and the corresponding value $\hat{q}$ of q is evaluated through the intersection method previously described. The value $\hat{\mu}$ of μ, corresponding to the couple $(\hat{p}, \hat{q})$ through equation (25), may be either larger or lower than the given μ. For the first frequency, if $\hat{\mu} > \mu$ then $p_u = \hat{p}$ if $\mu > 0{\cdot}17027$ or $p_l = \hat{p}$ if $\mu < 0{\cdot}17027$; otherwise, if $\hat{\mu} < \mu$ then $p_l = \hat{p}$ if $\mu > 0{\cdot}17027$ or $p_u = \hat{p}$ if $\mu < 0{\cdot}17027$. For all higher frequencies, it is $p_u = \hat{p}$ if $\hat{\mu} > \mu$ or $p_l = \hat{p}$ if $\hat{\mu} < \mu$. In this way, new upper and lower bounds are iteratively defined for p which, therefore, may be evaluated to the required degree of accuracy. The procedure will be terminated when

$$2(p_u - p_l)/(p_u + p_l) < \epsilon, \tag{27}$$

where ϵ is the permissible error.

6. NATURAL MODES OF VIBRATION

Natural modes of vibration are derived directly from the solution of the beam equation and are of the form

$$\phi_n(\zeta) = A_{1n} \sin b_n\zeta + A_{2n} \cos b_n\zeta + A_{3n} \sinh b_n\zeta + A_{4n} \cosh b_n\zeta, \tag{28}$$

where ζ is the dimensionless spatial co-ordinate z/L. The integration constants A_n are given by the expressions

$$A_{1n} = 1, \qquad A_{2n} = \frac{\mathrm{i}\mu b_n(\sin b_n - \sinh b_n)}{g}, \qquad A_{3n} = \frac{-2 \sin b_n + \mathrm{i}\mu b_n(\cos b_n - \cosh b_n)}{g}, \tag{29a–c}$$

$$A_{4n} = -A_{2n}, \qquad g = 2 \sinh b_n - \mathrm{i}\mu b_n(\cos b_n - \cosh b_n), \tag{30a, b}$$

obtained by applying the boundary conditions

$$v_A = 0, \qquad v_B = 0, \qquad M_A = -\mathrm{i}\omega c\varphi_A, \qquad M_B = -\mathrm{i}\omega c\varphi_B. \tag{31a–d}$$

It is worth noticing that the modes of vibration are complex and occur in conjugate pairs. One set of modes corresponds to the positive values of p_n, while the conjugate set corresponds to the negative ones.

7. ORTHOGONALITY CONDITIONS

The equations of motion for modes n and m are written as

$$EJ\phi_n'''' - \omega_n^2 m\phi_n = 0, \qquad EJ\phi_m'''' - \omega_m^2 m\phi_m = 0. \tag{32, 33}$$

By multiplying the first by ϕ_m and the second by ϕ_n and integrating between 0 and L, one obtains

$$\int_0^L EJ\phi_n''''\phi_m \,\mathrm{d}z - \omega_n^2 \int_0^L m\phi_n\phi_m \,\mathrm{d}z = 0,$$

$$\int_0^L EJ\phi_m''''\phi_n \,\mathrm{d}z - \omega_m^2 \int_0^L m\phi_n\phi_m \,\mathrm{d}z = 0. \tag{34, 35}$$

By integrating by parts and applying the boundary conditions, the previous equations may be written as

$$\int_0^L EJ\phi_n''\phi_m'' \,\mathrm{d}z + \mathrm{i}\omega_n c[\phi_n'(0)\phi_m'(0) + \phi_n'(L)\phi_m'(L)] - \omega_n^2 \int_0^L m\phi_n\phi_m \,\mathrm{d}z = 0, \tag{36}$$

$$\int_0^L EJ\phi_n''\phi_m'' \,\mathrm{d}z + \mathrm{i}\omega_m c[\phi_n'(0)\phi_m'(0) + \phi_n'(L)\phi_m'(L)] - \omega_m^2 \int_0^L m\phi_n\phi_m \,\mathrm{d}z = 0. \tag{37}$$

Subtraction of equation (36) from equation (37) provides

$$(\omega_n^2 - \omega_m^2) \int_0^L m\phi_n\phi_m \,\mathrm{d}z - \mathrm{i}c(\omega_n - \omega_m)[\phi_n'(0)\phi_m'(0) + \phi_n'(L)\phi_m'(L)] = 0, \tag{38}$$

which, for $\omega_n \neq \omega_m$, gives the first orthogonality condition

$$(\omega_n + \omega_m) \int_0^L m\phi_n\phi_m \, \mathrm{d}z - \mathrm{i}c[\phi_n'(0)\phi_m'(0) + \phi_n'(L)\phi_m'(L)] = 0. \tag{39}$$

By subtracting equation (36) multiplied by ω_m from equation (37) multiplied by ω_n, one obtains

$$(\omega_n - \omega_m)\omega_n\omega_m \int_0^L m\phi_n\phi_m \, \mathrm{d}z + (\omega_n - \omega_m) \int_0^L EI\phi_n''\phi_m'' \, \mathrm{d}z = 0, \tag{40}$$

which, for $\omega_n \neq \omega_m$, leads to the second orthogonality condition

$$\omega_n\omega_m \int_0^L m\phi_n\phi_m \, \mathrm{d}z + \int_0^L EI\phi_n''\phi_m'' \, \mathrm{d}z = 0. \tag{41}$$

8. MODAL DAMPING FACTORS

By setting $s_n = \mathrm{i}\omega_n$, the orthogonality conditions become

$$(s_n + s_m) \int_0^L m\phi_n\phi_m \, \mathrm{d}z + c[\phi_n'(0)\phi_m'(0) + \phi_n'(L)\phi_m'(L)] = 0, \tag{42}$$

$$s_n s_m \int_0^L m\phi_n\phi_m \, \mathrm{d}z - \int_0^L EI\phi_n''\phi_m'' \, \mathrm{d}z = 0. \tag{43}$$

Since to each eigenvalue s_n there corresponds the conjugate one $\bar{s}_n$, by taking $s_m = \bar{s}_n$ and by noticing that $s_n + \bar{s}_n = -2\xi_n|\omega_n|$ and $s_n\bar{s}_n = |\omega_n|^2$, it follows that

$$|\omega_n|^2 = \frac{\displaystyle\int_0^L EI|\phi_n''|^2 \, \mathrm{d}z}{\displaystyle\int_0^L m|\phi_n|^2 \, \mathrm{d}z} = \frac{k_n}{m_n}, \qquad 2\xi_n|\omega_n| = \frac{c[|\phi_n'(0)|^2 + |\phi_n'(L)|^2]}{\displaystyle\int_0^L m|\phi_n|^2 \, \mathrm{d}z} = \frac{c_n}{m_n}. \tag{44, 45}$$

Therefore, the damping mechanism may be idealized as a set of modal viscous dampers having a damping constant $c_n = c[|\phi_n'(0)|^2 + |\phi_n'(L)|^2]$. As a consequence, it is possible to define the modal damping factors ξ_n by equation (45).

9. COMPLEX MODE SUPERPOSITION METHOD

In the following sections the complex mode superposition method [1–4] for the dynamical analysis of the system under a transversal motion of both ends will be presented. At first, the modal impulsive response functions will be derived. Then these functions will be used to evaluate the response to a general seismic motion in the time and frequency domains.

9.1. MODAL IMPULSE RESPONSE FUNCTIONS

In the case of an impulsive transverse acceleration, acting at both ends simultaneously, the equation of motion takes the form

$$EJv''''(z, t) + m\ddot{v}(z, t) = -mI\delta(t), \tag{46}$$

where $I = \int_{0^-}^{0^+} \ddot{u}_g(t)\,\mathrm{d}t$ is the acceleration impulse and $\delta(t)$ is Dirac's delta function. In the mode superposition method, the response in terms of displacement can be expanded as a linear combination of modes of vibration as

$$v(z, t) = \sum_{n=1}^{\infty} y_n(t)\phi_n(z). \tag{47}$$

In this case, unlike the classical modal analysis, the vibration modes $\phi_n(z)$ are complex functions of the spatial co-ordinate z and the principal co-ordintates $y_n(t)$ are complex functions of time t. Due to the impulsive nature of the excitation, the principal co-ordinates take the form

$$y_n(t) = C_n \exp\{\mathrm{i}\omega_n t\}, \tag{48}$$

which imply

$$\dot{y}_n(t) = \mathrm{i}\omega_n y_n(t), \qquad \ddot{y}_n(t) = -\omega_n^2 y_n(t). \tag{49a, b}$$

By using the eigenfunction expansion, the equation of motion becomes

$$\sum_{n=1}^{\infty} [EJy_n(t)\phi_n''''(z) + m\ddot{y}_n(t)\phi_n(z)] = -mI\delta(t). \tag{50}$$

Multiplication by $\phi_m(z)$ and integration between 0 and L leads to

$$\sum_{n=1}^{\infty}\left[y_n(t)\int_0^L EJ\phi_n''''(z)\phi_m(z)\,\mathrm{d}z + \ddot{y}_n(t)\int_0^L m\phi_n(z)\phi_m(z)\,\mathrm{d}z\right] = -I\delta(t)\int_0^L m\phi_m(z)\,\mathrm{d}z. \tag{51}$$

Integrating by parts and applying the boundary conditions, one obtains

$$\sum_{n=1}^{\infty}\left\{y_n(t)\left[\mathrm{i}\omega_n c(\phi_n'(0)\phi_m'(0) + \phi_n'(L)\phi_n'(L)) + \int_0^L EJ\phi_n''(z)\phi_m''(z)\,\mathrm{d}z\right]\right.$$

$$\left. + \ddot{y}_n(t)\int_0^L m\phi_n(z)\phi_m(z)\,\mathrm{d}z\right\} = -I\delta(t)\int_0^L m\phi_m(z)\,\mathrm{d}z. \tag{52}$$

Upon making use of the orthogonality condition (39), the previous equation becomes

$$\sum_{n=1}^{\infty}\left\{y_n(t)\left[\mathrm{i}\omega_n c(\phi_n'(0)\phi_m'(0) + \phi_n'(L)\phi_m'(L)) - \omega_n\omega_m\int_0^L m\phi_n(z)\phi_m(z)\,\mathrm{d}z\right]\right.$$

$$\left. + \ddot{y}_n(t)\int_0^L m\phi_n(z)\phi_m(z)\,\mathrm{d}z\right\} = -I\delta(t)\int_0^L m\phi_m(z)\,\mathrm{d}z. \tag{53}$$

By using relationships (49) between the principal co-ordinates and their derivatives, after some algebraic manipulations, the following equation is found:

$$\sum_{n=1}^{\infty}\left\{\left[-\mathrm{i}c(\phi_n'(0)\phi_m'(0)+\phi_n'(L)\phi_m'(L))+(\omega_n+\omega_m)\int_0^L m\phi_n(z)\phi_m(z)\,\mathrm{d}z\right]\frac{\ddot{y}_n(t)}{\omega_n}\right\}$$

$$=-I\delta(t)\int_0^L m\phi_m(z)\,\mathrm{d}z. \quad (54)$$

It may be noted that, by applying the orthogonality condition (39), the expression in square brackets vanishes for $\omega_n \neq \omega_m$. Therefore the summation in the two previous equations reduces to only one term, making it possible to decouple the equations of motion which take the form

$$2\hat{M}_n\ddot{y}_n(t)+\hat{C}_n\ddot{y}_n(t)=-\hat{L}_nI\delta(t), \qquad n=1,2,\ldots, \quad (55)$$

where

$$\hat{L}_n=\int_0^L m\phi_n(z)\,\mathrm{d}z, \qquad \hat{M}_n=\int_0^L m\phi_n^2(z)\,\mathrm{d}z, \qquad \hat{C}_n=c(\phi_n'^2(0)+\phi_n'^2(L)). \quad (56a\text{–}c)$$

Integration of these equations in the time interval $[0^-, 0^+]$ leads to

$$2\hat{M}_n\dot{y}_n(0^+)+\hat{C}_ny_n(0^+)=-\hat{L}_nI, \quad (57)$$

from which the constants C_n are obtained:

$$C_n=-\frac{I\displaystyle\int_0^L m\phi_n\,\mathrm{d}z}{2\mathrm{i}\omega_n\displaystyle\int_0^L m\phi_n^2\,\mathrm{d}z+c(\phi_n'^2(0)+\phi_n'^2(L))}=IB_n. \quad (58)$$

The complex modal impulse response function may then be written as

$$h_n^c(z,t)=B_n\phi_n(z)\exp\{\mathrm{i}\omega_nt\}, \quad (59)$$

but the dynamic response can be evaluated more conveniently by using real algebra. This purpose can easily be achieved by summing each modal contribution to its conjugate one: i.e.,

$$h_n^r(z,t)=2\,\mathrm{Re}\,[B_n\phi_n(z)\exp\{\mathrm{i}\omega_nt\}]. \quad (60)$$

As a consequence, every modal impulsive response function is real and includes the contributions of both the mode and its conjugate. Although this function is formally real, it is still necessary to use complex algebra for its evaluation. However, by defining the real functions

$$\beta_n(z)=2\,\mathrm{Re}\,[B_n\phi_n(z)], \qquad \gamma_n(z)=2\,\mathrm{Im}\,[B_n\phi_n(z)], \qquad \alpha_n(z)=\xi_n\beta_n(z)-\sqrt{1-\xi_n^2}\gamma_n(z), \quad (61a\text{–}c)$$

the modal impulse response function may be expressed in terms of real algebra as

$$h_n^r(z,t)=\alpha_n(z)|\omega_n|h_n(t)+\beta_n(z)\dot{h}_n(t), \quad (62)$$

where

$$h_n(t) = (1/\omega_{Dn}) \exp\{-\xi_n|\omega_n|t\} \sin \omega_{Dn} t \tag{63}$$

represents the impulse response function of a single-degree-of-freedom linear viscous system with natural frequency $|\omega_n|$, damping ratio ξ_n and damped frequency $\omega_{Dn} = |\omega_n|\sqrt{1-\xi_n^2}$.

9.2. RESPONSE TO A GENERAL GROUND MOTION

By using the impulse response function (62), the dynamic response to a general ground motion may be obtained according to the modal superposition method as

$$v(z, t) = \sum_{n=1}^{\infty} \int_0^t \ddot{v}_g(\tau) h_n^r(z, t-\tau)\, \mathrm{d}\tau, \tag{64}$$

where the unitary impulse has been replaced by $I = \ddot{v}_g(\tau)\, \mathrm{d}\tau$ and the loading history has been divided into a sequence of impulses in the standard way of dynamic analysis. For computational purposes it is convenient to express the dynamic response in terms of response integrals as

$$v(z, t) = \sum_{n=1}^{\infty} [\alpha_n(z) V_n(t) + \beta_n(z) \dot{D}_n(t)], \tag{65}$$

where

$$V_n(t) = |\omega_n| D_n(t) = |\omega_n| \int_0^t \ddot{v}_g(\tau) h_n(t-\tau)\, \mathrm{d}\tau, \qquad \dot{D}_n(t) = \int_0^t \ddot{v}_g(\tau) \dot{h}_n(t-\tau)\, \mathrm{d}\tau. \tag{66, 67}$$

9.3. RESPONSE TO HARMONIC GROUND MOTIONS

When the ground motion is harmonic, the dynamic response may still be evaluated by means of equation (65), but the response integrals may be obtained in closed form as

$$D_n(t) = \frac{\exp\{\mathrm{i}\bar{\omega}t\} - [\cos \omega_{Dn} t + (\xi_n/\sqrt{1-\xi_n^2} + \mathrm{i}\bar{\omega}) \sin \omega_{Dn} t] \exp\{-\xi_n|\omega_n|t\}}{|\omega_n|^2 - \bar{\omega}^2 + \mathrm{i}2\xi_n|\omega_n|\bar{\omega}}\, \ddot{v}_{g0}, \tag{68}$$

$$\dot{D}_n(t) = \{\mathrm{i}\bar{\omega} \exp\{\mathrm{i}\bar{\omega}t\} + [\omega_{Dn} \sin \omega_{Dn} t + \xi_n|\omega_n| \cos \omega_{Dn} t - (\xi_n/\sqrt{1-\xi_n^2} + \mathrm{i}\bar{\omega}) \times (\omega_{Dn} \cos \omega_{Dn} t - \xi_n|\omega_n| \sin \omega_{Dn} t)] \exp\{-\xi_n|\omega_n|t\}\} \frac{\ddot{v}_{g0}}{|\omega_n|^2 - \bar{\omega}^2 + \mathrm{i}2\xi_n|\omega_n|\bar{\omega}}. \tag{69}$$

The steady-state response may then be evaluated by using the expressions

$$D_n(\bar{\omega}) = \frac{\ddot{v}_{g0}}{|\omega_n|^2 - \bar{\omega}^2 + \mathrm{i}2\xi_n|\omega_n|\bar{\omega}}, \qquad \dot{D}_n(\bar{\omega}) = \frac{\mathrm{i}\bar{\omega}\ddot{v}_{g0}}{|\omega_n|^2 - \bar{\omega}^2 + \mathrm{i}2\xi_n|\omega_n|\bar{\omega}}, \tag{70, 71}$$

which are obtained by removing the transient part from the response integrals (68) and (69).

10. NUMERICAL APPLICATIONS

The aim of the numerical applications reported here is to illustrate the main results derived in this paper. First of all, the results of a parametric study, which show the variation of natural frequencies as functions of the structural parameter μ, are presented.

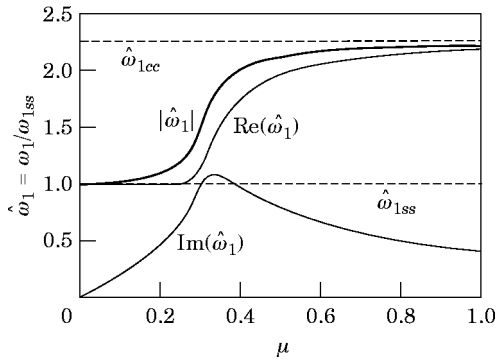

Figure 5. The real part (Re), imaginary part (Im) and modulus ($|\omega|$) of the first natural frequency as functions of the structural parameter μ. ω_{1ss} = first natural frequency of the simply supported beam; ω_{1cc} = first natural frequency of the beam with clamped ends.

Then, a graphical representation of a few nodal shapes is reported and the complex modal analysis is finally applied to evaluate the dynamic response to impulsive and harmonic excitations.

10.1. NATURAL FREQUENCIES

The modulus, the real and the imaginary parts of the first natural frequency are reported in dimensionless form in Figure 5 for $0 \leqslant \mu \leqslant 1$. It may be noted that the imaginary part, which is a measure of the amplitude decay of the modal motion, at first increases and reaches its maximum value for $\mu \simeq 0{\cdot}33$, then it decreases to zero as $\mu \to \infty$.

The real part, which has the physical meaning of a damped vibration frequency, remains approximately constant and slightly smaller than the first natural frequency of the simply supported beam when μ is less than about 0·22. Then it increases and tends asymptotically, like the modulus, to the value of the corresponding frequency of the beam with clamped ends.

The imaginary part and the modulus also present the same trend for higher frequencies, as may be seen from Figures 6 and 7 for the second and third frequencies, respectively. However, the real part starts to increase from the very beginning with increasing values of μ.

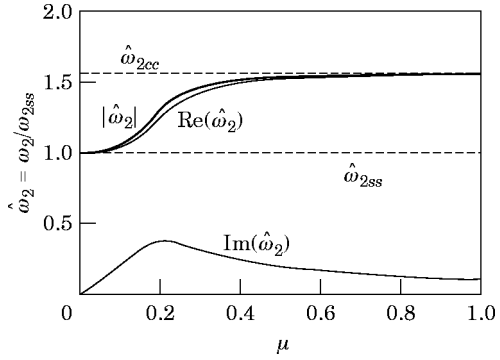

Figure 6. The real part (Re), imaginary part (Im) and modulus ($|\omega|$) of the second natural frequency as functions of the structural parameter μ. ω_{2ss} = second natural frequency of the simply supported beam; ω_{2cc} = second natural frequency of the beam with clamped ends.

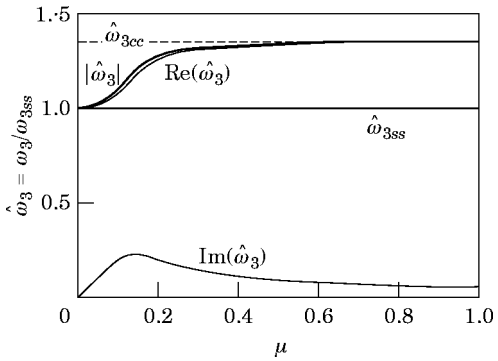

Figure 7. The real part (Re), imaginary part (Im) and modulus ($|\omega|$) of the third natural frequency as functions of the structural parameter μ. ω_{3ss} = third natural frequency of the simply supported beams; ω_{3cc} = third natural frequency of the beam with clamped ends.

From Figures 5, 6 and 7, it may be noted that increasing the damping parameter beyond a certain limit does not lead to an increase in the loss of energy but to a stiffening of the beam.

10.2. MODAL AMPLITUDE DECAY

As may be noted from the modal impulse response function $h_n(t)$, the reduction of a modal amplitude is related to the modal damping factor $\xi_n|\omega_n|$, which is actually the imaginary part of the complex natural frequency ω_n. The general picture of how this factor depends on the structural parameter μ is given in Figure 8 for the first three modes of vibration and for $0 \leqslant \mu \leqslant 1$. It may be seen that the modal amplitude decay factor increases with the mode order for $0 \leqslant \mu \leqslant 0{\cdot}36$ approximately.

For $\mu \geqslant 0{\cdot}36$ these factors practically coincide, showing that the amplitudes of all the modal contributions decrease at the same rate.

10.3. NATURAL MODES OF VIBRATION

The real and the imaginary parts of the first three modes of vibration are reported in Figure 9 for $\mu = 0{\cdot}20$. It may be noted that the real parts show a remarkable resemblance to the modes of the simply supported beam. The imaginary parts imply that all points of the beam vibrate out of phase in each modal contribution. This means that there are no nodes, i.e., points which do not move, and that the displacements at all points never vanish

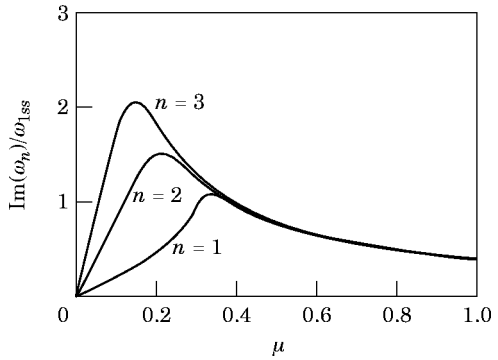

Figure 8. Amplitude decay factors for the first three modes as functions of the structural parameter μ.

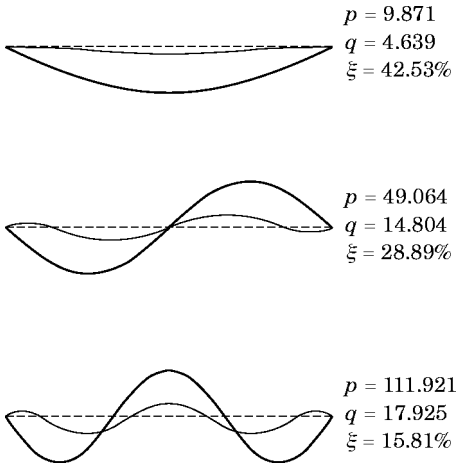

Figure 9. The real (heavy lines) and imaginary parts (light lines) of the first three modes of vibration of the system for $\mu = 0{\cdot}20$.

simultaneously nor reach their peak values at the same time. The modal shape changes within each period, but repeats itself with reduced amplitudes in the following periods.

When μ tends to infinity the imaginary parts vanish and the real parts coincide with the modal shape of the beam with clamped ends. For the sake of brevity, graphs showing this limiting case are not displayed.

10.4. TIME DOMAIN RESPONSE

The dynamic response to an impulse of transverse acceleration I, acting at both ends simultaneously, has been evaluated in terms of mid-span displacement and bending moment for $\mu = 0{\cdot}09$. The real and the imaginary parts of the first five frequency parameters have been reported in Table 1, together with the corresponding values of the damping factors. It may be noted that, in this case, the first modal damping factor is approximately 20%.

In Figure 10, the impulse modal response functions for the mid-span displacement, as defined in section 9.1, are reported for the first three conjugate pairs of vibration modes. It may be seen that the first modal contribution clearly prevails over the others and that, due to the dampers, the amplitude of all the displayed functions decays rapidly. In the same figure is also shown the impulse response function obtained by superposing the first five

TABLE 1

The first five frequency parameters and corresponding damping factors for $\mu = 0{\cdot}09$

Mode	p	q	ξ (%)
1	9·8608	1·8223	18·18
2	40·7014	7·3241	17·71
3	94·4598	15·7321	16·43
4	172·3820	24·4919	14·07
5	273·0706	31·0518	11·30

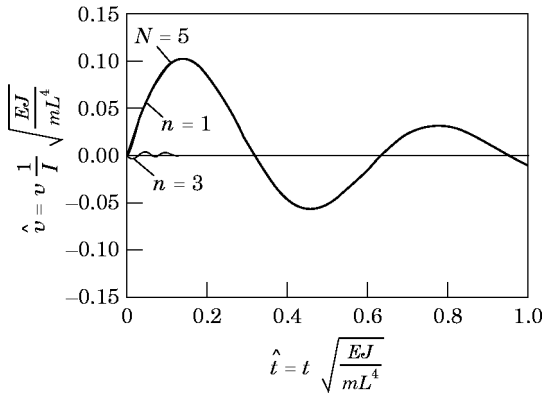

Figure 10. The modal impulse response functions for the mid-span displacement; $\mu = 0{\cdot}09$. ——, Modal impulse response function from the superposition of the first five modal responses.

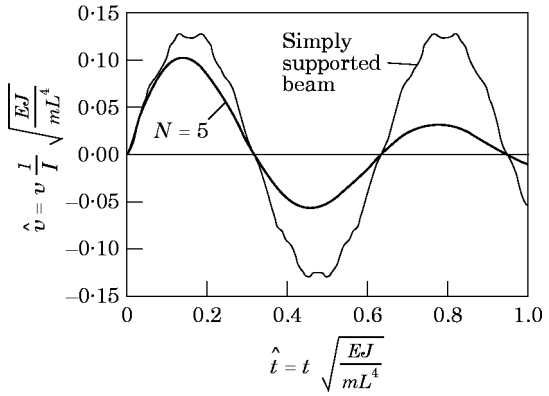

Figure 11. The modal impulse response functions for the mid-span displacement; $\mu = 0{\cdot}09$. ——, Beam with dampers; ——, beam without dampers.

modal contributions. This same function is also reported in Figure 11, where it may be compared with the corresponding one for the beam without dampers. A reduction of the maximum amplitude of about 25% may be clearly noted.

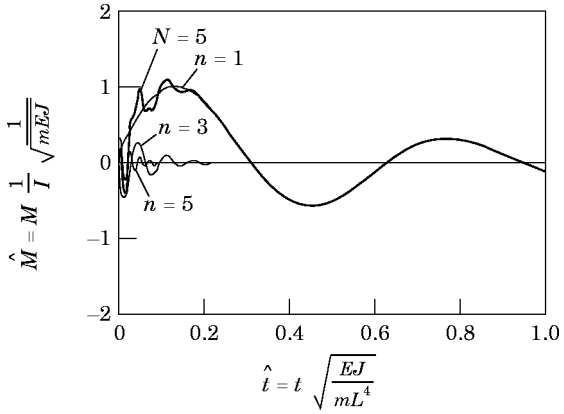

Figure 12. The modal impulse response functions for the mid-span bending moment; $\mu = 0{\cdot}09$. ——, Modal impulsive response function from the superposition of the first five modal responses.

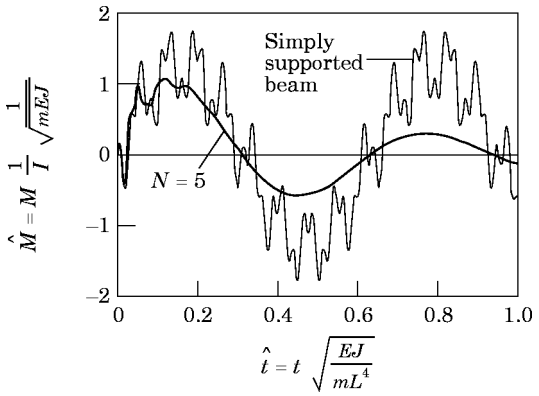

Figure 13. The modal impulse response functions for the mid-span bending moment; $\mu = 0{\cdot}09$. ——, Beam with dampers; ——, beam without dampers.

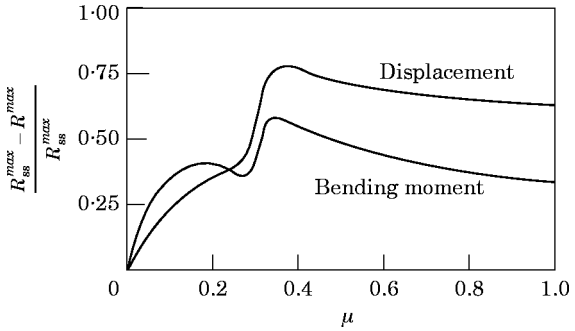

Figure 14. The maximum amplitude reduction of the impulse response functions for the mid-span displacement and bending moment as functions of the structural parameter μ. R^{max} = maximum response amplitude of the beam with dampers; R_{ss}^{max} = maximum response amplitude of the beam without dampers.

The mid-span bending moment shows the same trend, as may be seen in Figures 12 and 13. In this case the contribution of the higher modes is more important and the maximum amplitude reduction, being over 35%, is even more important.

The general picture of the maximum amplitude decrease is reported in Figure 14 for $0 \leqslant \mu \leqslant 1$. It may be noticed that the reduction reaches its maximum value when $\mu \simeq 0{\cdot}37$ for the mid-span displacement and when $\mu \simeq 0{\cdot}35$ for the mid-span bending moment. Such

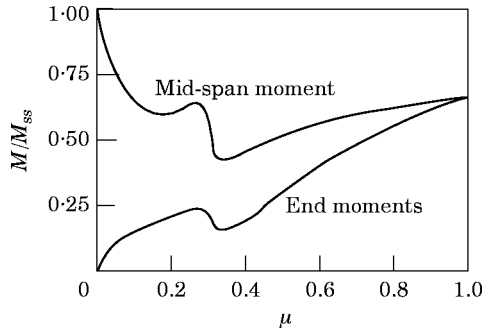

Figure 15. The ratio between the maximum moment, M, for the beam with dampers and the maximum mid-span moment, M_{SS}, for the beam without dampers.

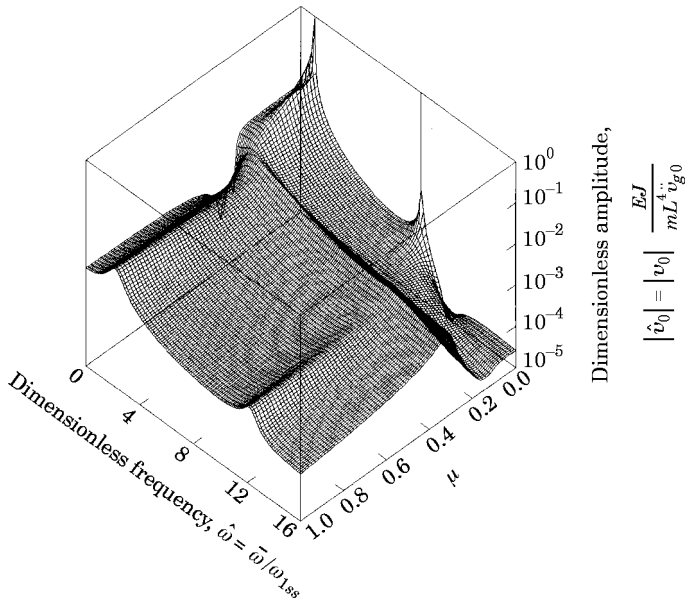

Figure 16. The amplitude of the frequency response function for the mid-span displacement.

a reduction appears to be very high, at about 80% for the displacement and 60% for the bending moment.

However, it should be noticed that, due to the presence of viscous dampers, together with the mid-span reduction, a bending moment arises at the ends of the beam. The ratio between the maximum amplitude of this bending moment and that at mid-span for the beam without dampers is shown in Figure 15 for $0 \leqslant \mu \leqslant 1$. The ratio between the maximum mid-span moments for the beam with and without dampers is also reported in Figure 15 for the sake of comparison. It may be noticed that as the mid-span moment

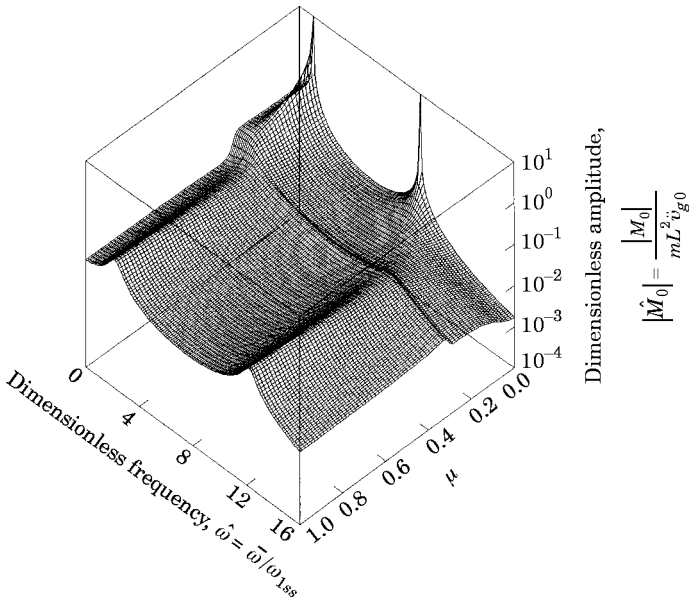

Figure 17. The amplitude of the frequency response function for the mid-span bending moment.

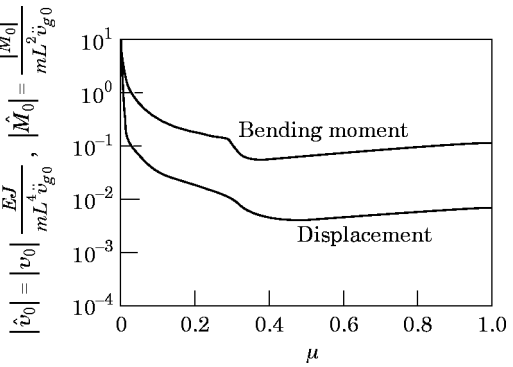

Figure 18. The first peak of the amplitude of the frequency response function for the mid-span displacement and bending moment.

decreases the end moments increase, but when the mid-span moment attains its absolute minimum the end moments reach a local minimum.

10.5. FREQUENCY DOMAIN RESPONSE

The amplitude of the frequency response function for the mid-span displacement is reported in Figure 16 for $0 \leqslant \mu \leqslant 1$. A similar representation for the mid-span bending moment is given in Figure 17. According to the results previously shown in Figures 5, 6 and 7, the peak amplitudes of both displacement and bending moment move to higher frequencies for increasing values of μ. The two ridges shown in Figures 16 and 17 correspond to the first and the third frequency as the contribution of the second frequency vanishes, because the excitation motion is symmetrical. The amplitudes of the first peak of the frequency response functions are reported in Figure 18 for $0 \leqslant \mu \leqslant 1$. It may be noted that the minimum displacement response is attained for $\mu = 0{\cdot}45$, while the minimum bending moment response occurs for $\mu = 0{\cdot}38$.

11. CONCLUSIONS

A numerical procedure for the evaluation of complex frequencies and modes of vibration of a simply supported beam with two rotational viscous dampers at its ends has been presented. The orthogonality conditions for decoupling the equation of motion have then been derived and complex modal analysis has been performed in order to evaluate the dynamical response to impulsive and harmonic transverse accelerations acting at both ends simultaneously.

Some numerical applications have pointed out that the dynamic response of structures designed as simply supported beams, such as bridges and long span roofs, can be considerably reduced by the use of rotational viscous dampers. An appropriate choice of the damper constant allows for the maximum reduction of the dynamic response or for an optimal overall design.

ACKNOWLEDGMENTS

This work has been financially supported by the Italian Ministry for University and Scientific and Technological Research (MURST).

REFERENCES

1. A. S. Veletsos and C. E. Ventura 1986 *Earthquake Engineering and Structural Dynamics* **14**, 217–243. Modal analysis of non-classically damped linear systems.
2. G. Oliveto and A. Santini 1994 *Proceedings of the Fifth International Conference on Recent Advances in Structural Dynamics*, *Southampton*, *England*, 775–784. Complex modal analysis of a soil–structure interacting model.
3. G. Oliveto and A. Santini 1996 *Journal of Sound and Vibration* **192**, 15–33. Complex modal analysis of a continuous model with radiation damping.
4. G. Oliveto and A. Santini 1996 *Engineering Structures* **18**, 425–436. Time domain response of a one-dimensional soil-structure interacting model via complex analysis.
5. R. Singh, W. M. Lyons and G. Prater 1989 *Journal of Sound and Vibration* **133**, 364–367. Complex eigensolution for longitudinally vibrating bars with a viscously damped boundary.
6. A. J. Hull 1994 *Journal of Sound and Vibration* **169**, 19–28. A closed form solution of a longitudinal bar with a viscous boundary condition.
7. J. H. B. Zarek and B. M. Gibbs 1981 *Journal of Sound and Vibration* **78**, 185–196. The derivation of eigenvalues and mode shapes for the bending motion of a damped beam with general end conditions.
8. R. W. Clough and J. Penzien 1975 *Dynamics of Structures*. New York: McGraw-Hill, first edition. See chapter 20.

APPENDIX A

The functions A, B, C and D, introduced in section 4, are given by the relationships

$$A = \frac{(EL + FL)c - (FL - EI)d}{L^2 + I^2}, \qquad B = \frac{(GL + HI)c - (HL - GI)d}{L^2 + I^2},$$

$$C = \frac{(EL + FL)d + (FL - EI)c}{L^2 + I^2}, \qquad D = \frac{(GL + HI)d + (HL - GI)c}{L^2 + I^2},$$

where

$$c = \mathrm{Re}\,[b] = \sqrt{\frac{p + \sqrt{p^2 + q^2}}{2}}, \qquad d = \mathrm{Im}\,[b] = \frac{q}{\sqrt{2(p + \sqrt{p^2 + q^2})}},$$

$$E = \cos d \cosh d(\sin c \cosh c - \cos c \sinh c) - \sin d \sinh d(\sin c \cosh c + \cos c \sinh c),$$

$$F = \sin d \cosh d(\sin c \sinh c - \cos c \cosh c) + \cos d \sinh d(\sin c \sinh c + \cos c \cosh c),$$

$$G = \cos d \sinh c - \sin c \cosh d, \qquad H = \sin d \cosh c - \cos c \sinh d,$$

$$I = \sin c \cos d \cosh c \sinh d - \cos c \sin d \sinh c \cosh d,$$

$$L = 1 - \cos c \cos d \cosh c \cosh d - \sin c \sin d \sinh c \sinh d.$$